NASA Technical Memorandum 82792

Analytical Investigation of Nonrecoverable Stall

Leon M. Wenzel and William M. Bruton
Lewis Research Center
Cleveland, Ohio

February 1982

NASA

ANALYTICAL INVESTIGATION OF NONRECOVERABLE STALL

by Leon M. Wenzel and William M. Bruton
National Aeronautics and Space Administration
Lewis Research Center
Cleveland, Ohio

SUMMARY

A lumped parameter model of the TF34 engine is formulated to study nonrecoverable stall. Features of the model include forward and reverse flow, radial flow in the fan, and variable corrected speed.

The purpose of the study is to point out those parameters to which recoverability is highly sensitive but are not well known. Experimental research may then be directed toward identification of the parameters in that category.

Compressor performance in the positive flow region and radial flow in the fan are shown to be important but unknown parameters determining recoverability. Other parameters such as compressor performance during reverse flow and in-stall efficiency have relatively small impact on recoverability.

INTRODUCTION

Compression system instability has received much attention over the past two decades. Intensive efforts in engine-inlet compatibility have done much to alleviate the problem of compressor stalls which was once quite serious.

However, as the incidence of inlet-induced stalls was reduced by improved design, the tendency was then to operate the compressor at increased pressure ratio to achieve greater performance. The cost of this increased performance is a loss in stall margin which implies again increased stall incidence. As a result, the industry has taken the point of view that occasional compressor stalls are an acceptable price for improved performance.

Many of the compressor stalls which occur recover, with only a momentary loss of power and without pilot action, and are of little consequence. Some stalls, however, cannot be cleared and are nonrecoverable. In these instances, the compressor settles into a stable operating point where it runs in rotating stall. Engine power output is very low, and internal temperatures are high enough to inflict damage. To recover from this condition, the engine must be shut down and restarted which requires deliberate pilot action and considerable time. Clearly, nonrecoverable stalls carry serious implications, and have been the object of intensive investigations in recent years.

The predominance of compressor mapping effort has been devoted to the unstalled region. Literature reporting in-stall compressor performance is sparse (see, for example, references 1 and 2). Greitzer, et al., in references 3 to 5 present data for several machines and suggest modelling techniques to accommodate post-stall operation.

The Air Force is currently contracting with General Electric and Pratt and Whitney to advance the technology in the nonrecoverable stall area. As a portion of their contract, GE has proposed to analyze TF34 data to be generated by LeRC. As a corollary to this TF34 experimental program, a post-stall model using characteristics specific to the TF34 has been developed. In this

report, the model is described, and results in terms of factors pertinent to recoverability from stall are given.

Description of Model

A lumped parameter representation of the TF34 engine system was developed on a hybrid computer. Performance parameters are included so that post-stall, as well as normal behavior is simulated. To facilitate observation of the rapidly occurring events which follow stall, the model is operated 1000 times slower than real time. A block diagram of the engine system model is shown in figure 1. In the sections which follow, descriptions will be given of the manner in which each component of the engine system is represented.

The symbols used in this report are defined in appendix A. A summary of equations is given in appendix B.

Compressor

The compressor is represented by overall maps, supplied by the manufacturer, with pressure ratio a function of corrected airflow. Fluid inertance is lumped, and compressor volume is divided between upstream and downstream stations. Mechanical speed is constant, but corrected speed varies.

In the performance map given, compressor pressure ratio varies approximately as $PNC^{5.5}$, (symbols are defined in appendix A) and corrected flow varies as PNC^{4}. This is contrary to incompressible theory in which corrected flow varies directly with speed, and pressure ratio varies as speed squared. A possible explanation for these unusual exponents is that the compressor variable geometry is scheduled as a function of corrected speed in this steady-state map.

The transients which are the subject of this study are rapid. It is judged that: 1) corrected speed cannot be sensed and computed that rapidly by the engine control system, and 2) the variable geometry actuators would be unable to respond quickly. Hence, the variable geometry would remain relatively fixed, and the reported map would not be valid. Accordingly, the speed line for PNC = 1. is used as a baseline. Other speed lines are obtained by shifting the PNC = 1 line by conventional incompressible theory; pressure ratio is shifted as PNC^{2}, and corrected flow as PNC.

In this approach, an in-stall pressure parameter ψ, proportional to downstream static pressure minus upstream total pressure divided by inlet density times wheel speed squared, is calculated as a function of a flow parameter ϕ, proportional to flow velocity divided by wheel speed. Greitzer suggests a numerical value for the pressure parameter at zero flow based on observations of several machines. For non-zero flows, both positive and negative, a parabolic relationship is assumed where ψ varied as ϕ^{2}, and the proportionality constant is treated parametrically.

The pressure parameter used is based on compressor downstream static pressure. Downstream total pressure is calculated by multiplying the downstream static pressure by a constant. Since compressor discharge mach number is always low, errors introduced by this simplification are minor.

Hysteresis exists in the compressor stall/recovery process. The operating point and the stalling flow are known. The value of flow at which recovery occurs is chosen to be greater than operating point flow, and is varied parametrically. The compressor map which results is shown in figure 2. In this

figure, speed lines for PNC = 0.8, 0.9 and 1. indicate how performance shifts with corrected speed.

When flow through the compressor reverses, the compressor inlet reference station is switched from the volume at the compressor inlet to the burner volume. Compressor flow is then corrected by conditions in the burner. The correcting factor for compressor speed is not switched to burner temperature because that would result in an undesireable discontinuity at zero flow, and because data indicate that rotational speed is unimportant during reverse flow.

Temperature performance in the in-stall, positive flow region is calculated from the pressure performance described above and hypothesized efficiency. Recent unpublished compressor rig data indicate a smooth transition in temperature ratio when going from unstalled to stalled operation. The stalled efficiency is based on the value required to achieve this smooth transition in temperature ratio when going from unstalled to stalled operation and some low value at zero flow, with linear interpolation between. The zero flow efficiency is treated parametrically. Resulting temperature ratio characteristics, for PNC = 1. and several zero flow efficiencies are given in figure 3.

Fan

The fan is treated in a similar, but simpler, manner as the compressor. Unstalled performance is obtained from reference 6. Stalled performance is handled as in the compressor. For the fan, temperature ratio is assumed constant.

Two fan maps, one for the hub and one for the tip are used, and are presented in figure 4. Radial crossflow between hub and tip regions is allowed, proportional to the pressure difference. Since the tip pressure ratio is slightly higher than the hub pressure ratio, a constant pressure source (linear map) is added in the hub to tip flow path. This is adjusted for zero quiescent cross flow. The flow impedance between the hub and tip regions is varied parametrically.

Combustor

The combustor is modelled simply. Heat is released as soon as fuel enters the combustor. During periods of reduced or reversed airflow, the mixture in the combustor becomes very rich because of the relatively slow fuel system dynamics. Instantaneous fuel-air ratio of the gases in the combustor is computed. If this ratio exceeds the stoichiometric ratio, only that portion of fuel for which the necessary air is present is allowed to react.

Volume Dynamics

Pressures and temperatures within the lumped volumes are computed using well established techniques (e.g., reference 7). For temperature determination during reverse flow, the temperature multiplier is switched from the normal entering value to that of the volume(e.g., eq. B3). This has the effect of bleeding energy from the downstream volume and heating the inlet volume.

Rotational Speed

The model does not include turbines or rotor dynamics; mechanical speed is constant. However, the reversed flow of hot gases raised the inlet temperature to the compressor and fan, which causes their corrected speeds to decrease. This phenomenon is modeled.

Control

The fuel control is simply a constant W_f/P_3, with no dynamics. Fuel pulse disturbances are introduced by programming a false P_3, which is common test-cell practice.

Compressor variable geometry is not modeled, as discussed earlier.

Analytical Investigation

The model is exercised to assess the importance of various parameters on the recoverability of the system following a compressor stall. Two procedures are required; one to stall the compressor and one to rate the stability of the system.

Compressor stall is effected by fuel pulses. A false burner pressure signal is applied to the simplified control wherein W_f/P_3 is constant. Fuel flow is ramped up to a value just sufficient to cause stall and is then ramped down to a minimum value. Equal times (0.010 sec.) are used for the ramp up and the ramp down.

Turbine area is used as a stability rating criterion. At the time of compressor stall, turbine area is reset by some increment which can be positive or negative. This increment is adjusted until the compressor just recovers. For the nominal case, this area is defined as $\overline{A}$. Then some parameter is changed and a new recovery area identified by trial and error. A change in area is then defined as $\Delta A = A_{new} - \overline{A}$. If the new area is larger than $\overline{A}$, the parameter change has had a detrimental effect on recovery. Hence, positive $\Delta A/\overline{A}$ is bad.

Examples of transients which did and did not recover, plotted on a compressor map, are presented in figure 5.

Results and Discussion

A set of system parameters is chosen for a nominal case. The nominal case has positive recovery margin so that the turbine area required for recovery is less than its nominal value at the operating point. Many of the system parameters have to do with engine geometry and can be measured or calculated with reasonable assurance. Several parameters, however, are unknown and were necessarily chosen in an arbitrary manner. It is a purpose of this investigation to study the sensitivity of stall recovery to system parameters, especially those which are nebulous. In this way, experimental effort can be directed toward the evaulation of those parameters which are not well known but are nevertheless important.

Some of these parameters will be discussed individually as warranted; the recovery sensitivities of all the parameters will be summarized.

Compressor In-Stall Performance

In the in-stall positive flow region the pressure coefficient was modeled as $\psi_C = KPC\ \phi_C^2 + 1.54$ where ϕ_C is the flow coefficient, 1.54 is the value of ψ_C at zero flow suggested by Greitzer, and KPC is a parametrically varied constant. A similar relationship is used in the negative flow region, $\psi_C = KNC\ \phi_C^2 + 1.54$.

Recovery is very sensitive to KPC (figure 6). The reason for this can be understood by referring back to figure 5. Results indicate that, for recovery, the trajectory should not intersect the in-stall characteristic in the positive flow region. The trajectory should remain below the in-stall characteristic at least until the flow at which recovery occurs is reached. (It must be kept in mind that PNC along the trajectory, and is generally not on one of the speed lines shown. For the recovering transient, PNC is approximately 0.87 at recovery.) Since the slopes of the trajectory and the characteristic are similar an increase in the value of the characteristic would result in a significant decrease in the throttle area necessary to avoid intersection.

Recovery is much less sensitive to the characteristic in the negative flow region, determined by KNC. The recovery sensitivities can be expressed as the slopes of the sensitivity plots in figure 6 at the origin. The values

calculated from figure 6 are $\frac{\Delta(\Delta A/\overline{A})}{\Delta(\Delta KPC/\overline{KPC})} = 1.35$, and $\frac{\Delta(\Delta A/\overline{A})}{\Delta(\Delta KNC/\overline{KNC})} = 0.05$.

A qualitative idea of this great difference in sensitivity is given in figure 7. In the positive flow region, the nominal characteristic is the $\Delta A/\overline{A} = 0$ curve. Above and below the nominal, characteristics corresponding to -10 percent and +10 percent $\Delta A/\overline{A}$, respectively, are shown. In the negative flow region, the nominal characteristic is shown together with that for $\Delta A/\overline{A} = +10$ percent. It is clear that a minute change in the positive-flow stalled characteristic is equivalent to a large change in the negative-flow stalled characteristic.

Fan Radial Flow

Communication between the hub and tip regions of the fan has received much interest. Proximate splitters have been proposed and tried to prevent augmentor ignition pulses from entering the core.

Flow in the radial direction is assumed to vary linearly with the pressure difference. A nominal value of flow resistance is arbitrarily chosen to be (0.01 lbf sec/lbm in^2). Since so little was known of the numerical value of this resistance, it is varied over a wide range.

The recovery area required for a range of radial flow resistances is plotted in figure 8. The curve is neither monotonic nor linear, but the general trend is toward less likely recovery as radial flow resistance is increased.

Compressor Efficienty at Zero Flow

Compressor efficiency is handled as previously described; arbitrarily chosen at zero flow and as required for a smooth temperature transition at

stall. The zero flow efficiency is found to have a relatively minor effect on recovery area.

Fan Inlet Volume

The forward boundary conditions are established by the volume at the fan entrance, and by the source impedance through which this volume communicates with the ambient. Since these parameters are unknown, they are varied over wide ranges. Recovery area is slightly affected by fan inlet geometry.

Other Effects

Table I summarizes the sensitivity of recovery area to all of the parameters which were investigated. The results are tabulated as the slope of the function at the nominal point. The results are listed in order of decreasing sensitivity. A positive sign indicates that an increase in the value of the parameter has a detrimental effect on recovery, i.e., more turbine area is required for recovery.

Again, one of the intents of this study is to point out areas which require further definition. In table I, some of the parameters high on the list, e.g., compressor discharge volume and inertance, involve engine geometry and may be readily evaluated. Others, e.g., compressor pressure performance at negative flow and compressor stall/recovery hysteresis, are not well known but are relatively unimportant to the recovery process.

Of concern are those parameters which are not known but are highly sensitive. Prime examples of these are compressor performance in the positive flow region and the resistance to flow between the fan hub and tip regions. Although these parameters will be difficult to measure experimentally, they are requisite for a meaningful engine system model.

SUMMARY

A lumped parameter model of the TF34 engine is formulated. Features of the model include forward and reverse flow through the machine, radial flow in the fan and variable corrected speeds. In-stall compression system performance is necessarily hypothesized. Both recoverable and non-recoverable stall behavior are exhibited by the model.

A study is conducted in which several system parameters are varied to determine their effect on recoverability. System stability is rated on the turbine area necessary to recover; a more stable system recovers with a smaller turbine area.

The purpose of the study is to point out those parameters to which recoverability is highly sensitive but are not well known. Experimental research may then be directed toward identification of the parameters in that category.

Examples of parameters sensitive but unknown are compressor performance in the positive flow region and radial flow in the fan. Other parameters such as compressor performance during reverse flow and in-stall efficiency have relatively small impact on recoverability.

REFERENCES

1. Emmons, H.W.; Pearson C.E.; and Grant, H.P.: Compressor Surge and Stall Propagation. Trans. ASME, vol. 77, Apr. 1955, pp.455-469.
2. Iura, T.; and Rannie, W.D.: Experimental Investigations of Propagating Stall in Axial-Flow Compressors. Trans ASME, vol. 76, Apr. 1954, pp. 463-471.
3. Day, I.J.; Greitzer, E.M.; and Cumpsty, N.A.: Prediction of Compressor Performance in Rotating Stall. J. Eng. Power, vol. 100, no. 1, Jan. 1978, pp. 1-14.
4. Greitzer, E.M.: Surge and Rotating Stall in Axial Flow Compressors. Part I: Theoretical Compression System Model. ASME Paper 75-GT-9, Mar. 1975.
5. Greitzer, E.M.: Surge and Rotating Stall in Axial Flow Compressors. Part II: Experimental Results and Comparison With Theory. ASME Paper 75-GT-10, Mar. 1975.
6. Hosny, W.M.; Steenken, W.G.: TF34 Engine Compression System Computer Study - Simulation of Flow Stability. (R78AEG612, General Electric Co.; NASA Contract NAS3-20599.) NASA CR-159889, 1979.
7. Seldner, Kurt; Mihaloew, James R.; and Blaha, Ronald J.: Generalized Simulation Technique for Turbojet Engine System Analysis. NASA TN D-6610, 1972.

APPENDIX A
SYMBOLS

A	area	in^2	m^2
a	constant in linearization of C_p	Btu/lbm $°R^2$	J/kg K^2
b	constant in linearization of C_p	Btu/lbm °R	J/kg K
C_p	specific heat at constant pressure	Btu/lbm °R	J/kg K
dt	time increment	sec	sec
F_i	performance function (i = 1,4)	–	–
G	function	–	–
H	enthalpy	Btu/lbm	J/kg
h	heat transfer coefficient	Btu/in^2 sec °R	J/m^2 sec K
HV	heating value of fuel	Btu/lbm	J/kg
K	constant	–	–
KNC	constant describing in-stall compressor performance at negative flow	–	–
KNF	constant describing in-stall fan performance at negative flow	–	–
KPC	constant describing in-stall compressor performance at positive flow	–	–
KPF	constant describing in-stall fan performance at positive flow	–	–
L	fluid inertance, length/(area g)	sec^2/in^2	sec^2/m^2
N	rotational speed	rev/min	rev/min
p	static pressure	lbf/in^2	N/m^2
P	total pressure	lbf/in^2	N/m^2
PNC	fractional corrected compressor speed	–	–
PNF	fractional corrected fan speed	–	–
Q	heat flux	Btu/sec	J/sec
$\mathscr{R}$	gas constant	in lbf/lbm °R	N m/kg K
R	flow resistance, Δ (pressure drop)/ Δ (flow)	lbf sec/lbm in^2	N sec/kg m^2
T	temperature	°R	K
t	time	sec	sec
V	volume	in^3	m^3
W	weight	lbm	kg
$\dot{W}$	weight flow	lbm/sec	kg/sec
α	constant	–	–
γ	ratio of specific heats	–	–
δ	ratio of total pressure to standard atmospheric pressure	–	–
Δ	incremental change	–	–
η	efficiency	–	–
θ	ratio of total temperature to standard atmosphereic temperature	–	–
ϕ	flow parameter	–	–
ψ	pressure parameter	–	–

Subscripts:

0	ambient
1	fan inlet
2	compressor
2H	fan hub discharge
2T	fan tip discharge
3	compressor discharge
air	air
as	air, stored
ave	average
C	compressor
D	design
duct	duct
exit	exit
F	fan
f	fuel
fb	burned fuel
fs	unburned fuel stored in combustor
i	initial
H	fan hub
metal	compressor metal
S	standard
T	fan tip
X	fan radial flow

Superscripts:

'	denotes parameter switched during flow reversal
-	Nominal
*	denotes quasi-steady parameter at compression component discharge

Constants:

KNC	50.	nominal values
KNF	5.	
KPC	5.	
KPF	0.5	
R_0	1.644×10^{-3}	
R_{duct}	0.02715	
R_X	0.01	

APPENDIX B
SUMMARY OF EQUATIONS

NOTE: The terms within braces { } in the equations were switched when flow reversed. If flow was positive, in the normal sense, the upper term within the braces was used. The equations in which this applies are B3, B11 B20, B25, B31, B32, B35, B39, B40, B47, and B51.

Fan Inlet

$$\dot{W}_0 = \frac{P_0 - P_1}{R_0} \tag{B1}$$

$$W_1 = \int_0^t (\dot{W}_0 - \dot{W}_T - \dot{W}_H)\, dt + W_{1,i} \tag{B2}$$

$$(WT)_1 = \gamma \int_0^t \left(\dot{W}_0 \begin{Bmatrix} T_0 \\ T_1 \end{Bmatrix} - \dot{W}_T \begin{Bmatrix} T_1 \\ T_{2T} \end{Bmatrix} - \dot{W}_H \begin{Bmatrix} T_1 \\ T_{2H} \end{Bmatrix} \right) dt + (WT)_{1,i} \tag{B3}$$

$$P_1 = \frac{\mathscr{R}(WT)_1}{V_1} \tag{B4}$$

$$T_1 = \frac{(WT)_1}{W_1} \tag{B5}$$

$$\dot{W}_1 = \dot{W}_T + \dot{W}_H \tag{B6}$$

$$\theta_1 = \frac{T_1}{T_S} \tag{B7}$$

$$\delta_1 = \frac{P_1}{P_S} \tag{B8}$$

$$PNF = \frac{N_F/\sqrt{\theta_1}}{\left(N_F/\sqrt{\theta_1}\right)_D} \tag{B9}$$

$$\phi_F = 3.594 \times 10^{-3} \frac{\dot{W}_1\sqrt{\theta_1}/\delta_1}{PNF} \tag{B10}$$

$$\psi_F = \left\{ \begin{matrix} KPF \\ KNF \end{matrix} \right\} \phi_F^2 + 0.11 \tag{B11}$$

Fan Discharge

Unstalled

$$\frac{P^*_{2T}/P_1 - 1}{PNF} = F_1\left(\frac{W_1\sqrt{\theta_1}/\delta_1}{PNF}\right)$$

$$\frac{P^*_{2H}/P_1 - 1}{PNF} = F_2\left(\frac{W_1\sqrt{\theta_1}/\delta_1}{PNF}\right)$$

Stalled

$$P^*_{2T} = 1.073\, P_1\left(1 + \frac{PNF^2}{0.9916}\,\psi_F\right) \tag{B12}$$

$$P^*_{2H} = 1.073\, P_1\left(1 + \frac{PNF^2}{0.9916}\,\psi_F\right) \tag{B13}$$

$$T^*_{2T} = 1.11\, T_1 \tag{B14}$$

$$T^*_{2H} = 1.11\, T_1 \tag{B15}$$

$$\dot{W}_T = \frac{1}{L_T}\int_0^t \left(P^*_{2T} - P_{2T}\right) dt + \dot{W}_{T,i} \tag{B16}$$

$$\dot{W}_H = \frac{1}{L_H}\int_0^t \left(P^*_{2H} - P_{2H}\right) dt + \dot{W}_{H,i} \tag{B17}$$

Fan Duct Inlet

$$\dot{W}_{duct} = \frac{1}{R_{duct}} (P_{2T} - P_{exit}) \tag{B18}$$

$$W_{2T} = \int_0^t (\dot{W}_T - \dot{W}_X - \dot{W}_{duct})\, dt + W_{2T,i} \tag{B19}$$

$$(WT)_{2T} = \gamma \int_0^t \left(\dot{W}_T \begin{Bmatrix} T^*_{2T} \\ T_{2T} \end{Bmatrix} - \dot{W}_X \begin{Bmatrix} T_{2T} \\ T_{2H} \end{Bmatrix} - \dot{W}_{duct}\, T_{2T} \right) dt + (WT)_{2T,i} \tag{B20}$$

$$P_{2T} = \frac{\mathcal{R}(WT)_{2T}}{V_T} \tag{B21}$$

$$T_{2T} = \frac{(WT)_{2T}}{W_{2T}} \tag{B22}$$

Compressor Inlet

$$\dot{W}_X = \frac{1}{R_X} (P_{2T} - P_{2H} - P_X) \tag{B23}$$

$$W_{2H} = \int_0^t (\dot{W}_H - \dot{W}_2 + \dot{W}_X)\, dt = W_{2H,i} \tag{B24}$$

$$(WT)_{2H} = \gamma \int_0^t \left(\dot{W}_H \begin{Bmatrix} T^*_{2H} \\ T_{2H} \end{Bmatrix} - \dot{W}_2 \begin{Bmatrix} T_{2H} \\ T_3 \end{Bmatrix} + \dot{W}_X \begin{Bmatrix} T_{2T} \\ T_{2H} \end{Bmatrix} - \frac{Q_{metal}}{C_{P_{air}}} \right) dt + (WT)_{2H,i} \tag{B25}$$

$$P_{2H} = \frac{\mathcal{R}(WT)_{2H}}{V_H} \tag{B26}$$

$$T_{2H} = \frac{(WT)_{2H}}{W_{2H}} \tag{B27}$$

$$Q_{metal} = hA\ (T_{2H} - 1.11\ T_0) \tag{B28}$$

$$\dot{W}_2 = \frac{1}{L_C} \int_0^t (P_3^* - P_3)\ dt + \dot{W}_{2,i} \tag{B29}$$

$$\theta_{2H} = \frac{T_{2H}}{T_S} \tag{B30}$$

$$\theta'_{2H} = \frac{\left\{ \begin{matrix} T_{2H} \\ T_3 \end{matrix} \right\}}{T_S} \tag{B31}$$

$$\delta_{2H} = \frac{\left\{ \begin{matrix} P_{2H} \\ P_3 \end{matrix} \right\}}{P_S} \tag{B32}$$

$$PNC = \frac{N_C/\sqrt{\theta_{2H}}}{(N_C/\sqrt{\theta_{2H}})_D} \tag{B33}$$

$$\phi_C = 3.779 \times 10^{-2}\ \frac{\dot{W}_2 \sqrt{\theta'_{2H}}/\delta_{2H}}{PNC} \tag{B34}$$

$$\psi_C = \left\{ \begin{matrix} KPC \\ KNC \end{matrix} \right\} \phi_C^2 + 1.54 \tag{B35}$$

Compressor Discharge

Unstalled

$$\frac{P_3^*/P_{2H} - 1}{PNC^2} = F_3\left(\frac{\dot{W}_2\sqrt{\theta_{2H}}/\delta_{2H}}{PNC}\right)$$

Stalled

$$P_3^* = 1.026\, P_{2H}\,(1 + 0.8528\, PNC^2\, \psi_C) \tag{B36}$$

$$\frac{T_3^*/T_{2H} - 1}{PNC^2} = F_4\left(\frac{\dot{W}_2\sqrt{\theta_{2H}}/\delta_{2H}}{PNC}\right)$$

$$T_3^* = T_{2H}\left(1 + PNC^2\,\frac{(P_3^*/P_{2H})^{(\gamma - 1)/\gamma} - 1}{\eta}\right) \tag{B37}$$

$$\eta = \alpha\phi_C + \eta\Big|_{\phi_C = 0} \tag{B38}$$

Combustor

$$W_{as} = \int_0^t \left[\begin{Bmatrix}\dot{W}_2\\ 0\end{Bmatrix} - \frac{1}{f/a + 1}\left(\dot{W}_3 - \begin{Bmatrix}0\\ \dot{W}_2\end{Bmatrix}\right)\right] dt + W_{as,i} \tag{B39}$$

$$W_{fs} = \int_0^t \left[\dot{W}_f - \frac{f/a}{f/a + 1}\left(\dot{W}_3 - \begin{Bmatrix}0\\ \dot{W}_2\end{Bmatrix}\right)\right] dt + W_{fs,i} \tag{B40}$$

$$f/a = \frac{W_{fs}}{W_{as}} \tag{B41}$$

$$G = 1 - \frac{a/f}{15} \qquad (G \geq 0) \tag{B42}$$

$$\dot{W}_f = \dot{W}_{fD} + \left(\frac{\dot{W}_f}{P_3}\right)_D F(t) \tag{B43}$$

$$\dot{W}_{fb} = (1 - G)\,\dot{W}_f \tag{B44}$$

$$Q = 0.95\ HV\ \dot{W}_{fb} \tag{B45}$$

$$P_3 = \frac{\mathcal{R} T_3 (W_{as} + W_{fs})}{V_3} \tag{B46}$$

$$(WH)_3 = \gamma \int_0^t \left(C_p \dot{W}_2 \begin{Bmatrix} T_3^* \\ T_3 \end{Bmatrix} - C_p \dot{W}_3 T_3 + Q \right) dt + (WH)_{3,i} \tag{B47}$$

$$H_3 = \frac{(WH)_3}{W_{as} + W_{fs}} \tag{B48}$$

$$T_3 = \frac{H_3}{C_p} \tag{B49}$$

$$T_{ave} = \frac{T_3^* + T_3}{2} \tag{B50}$$

$$C_p = a \begin{Bmatrix} T_{ave} \\ T_3 \end{Bmatrix} + b \tag{B51}$$

$$\dot{W}_3 = K \left(1 + \Delta A \right) \frac{P_3}{\sqrt{T_3}} \tag{B52}$$

TABLE I. - SENSITIVITY OF SMALL RECOVERY AREA TO VARIOUS SYSTEM PARAMETERS

Parameter X	$\left.\frac{\Delta(\Delta A/\bar{A})}{\Delta(\Delta X/\bar{X})}\right\|_{\frac{\Delta X}{\bar{X}}=0}$
Compressor discharge volume	-1.67
KPC, compressor positive flow pressure performance	-1.35
Compressor inertance	+0.97
Fan exhaust duct ΔP	-0.83
Fan tip discharge volume	+0.56
Fan inertance	+0.38
Fan radial flow resistance	+0.24
Fan hub discharge volume	+0.20
Fan inlet volume	-0.12
Compressor η at zero flow	-0.09
KNC, compressor negative flow pressure performance	+0.05
Fan inlet duct ΔP	-0.04
Compressor hysteresis	+0.03

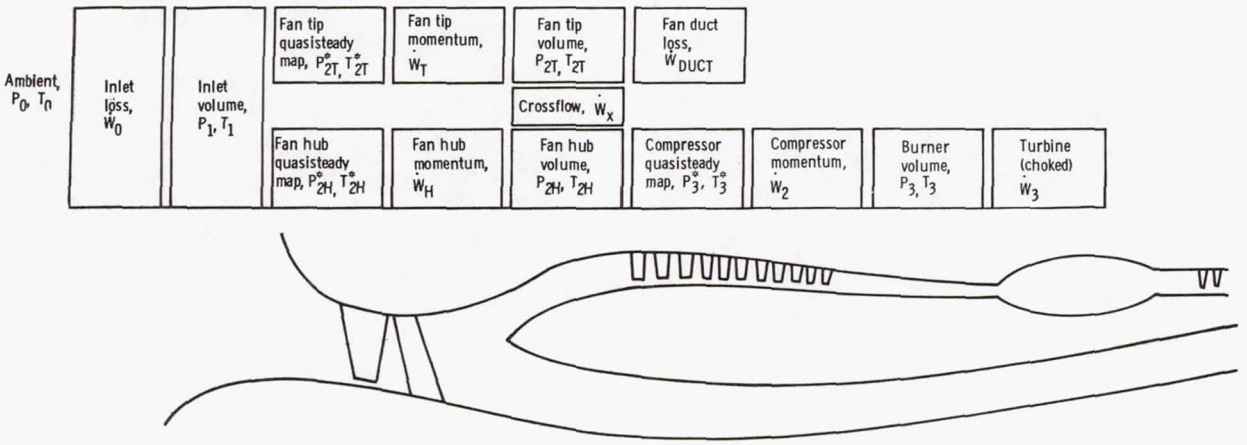

Figure 1. Block diagram of engine system model.

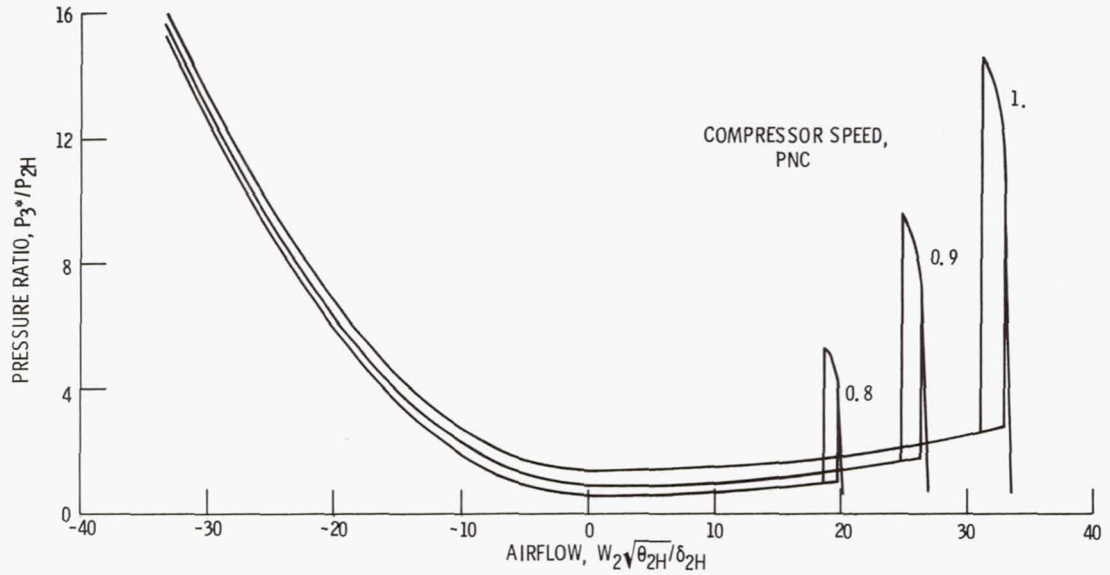

Figure 2. - Pressure performance map for compressor.

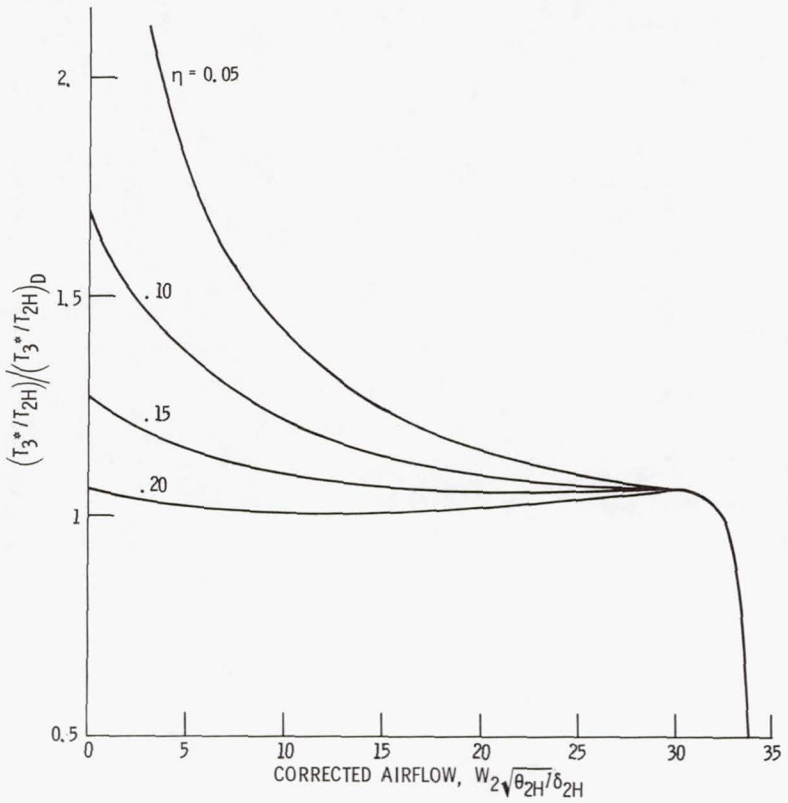

Figure 3. - Temperature performance maps for compressor with various zero-flow efficiencies.

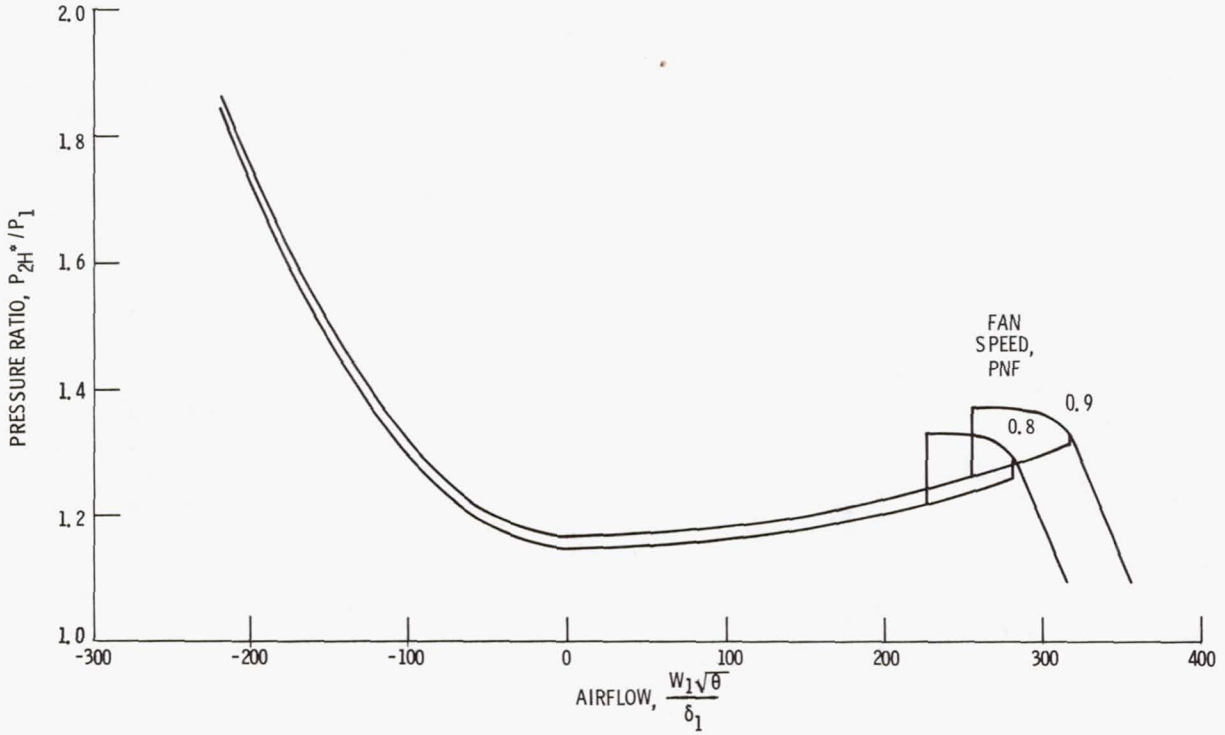

(a) Fan hub.

Figure 4. - Pressure performance map.

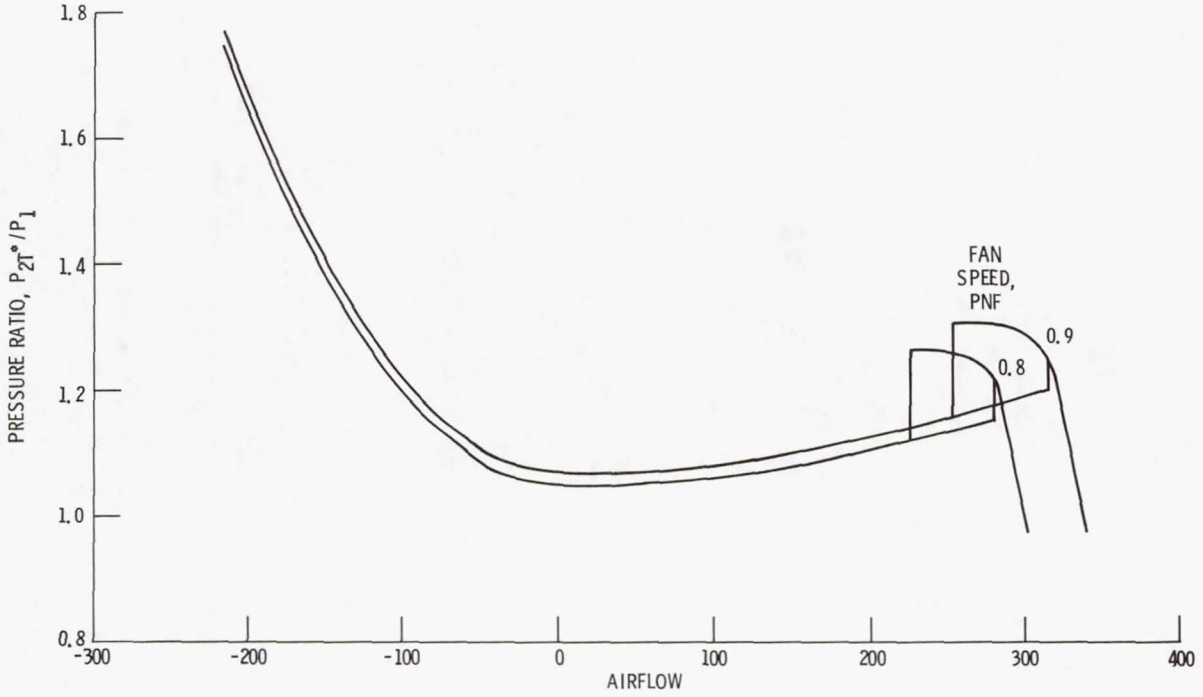

(b) Fan tip.

Figure 4. - Concluded.

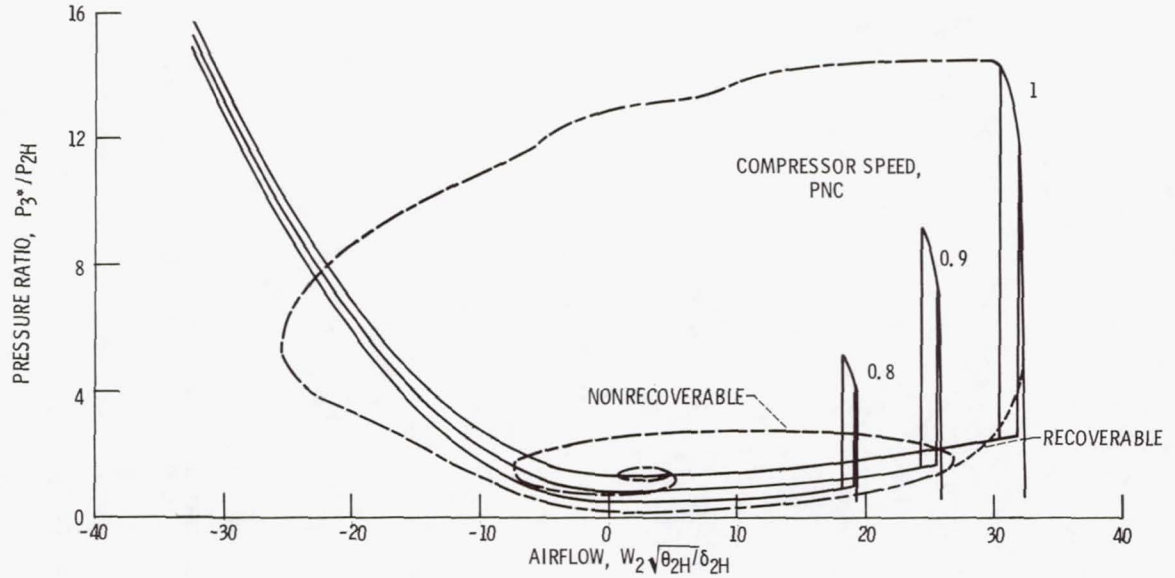

Figure 5. - Trajectories of recoverable and nonrecoverable transients.

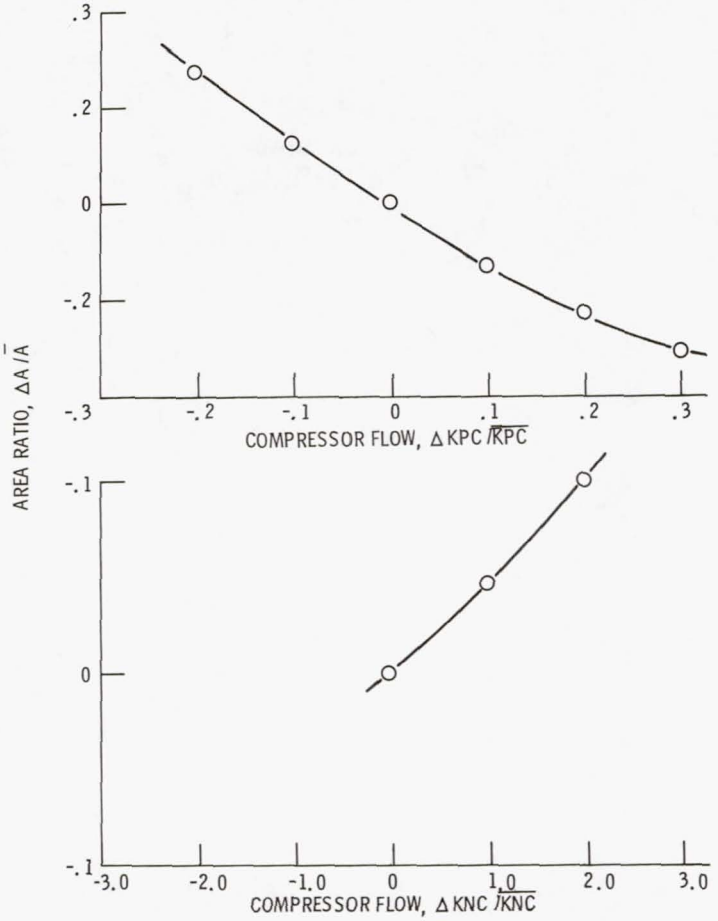

Figure 6. - Variation in recovery area as a function of compressor install performance coefficients.

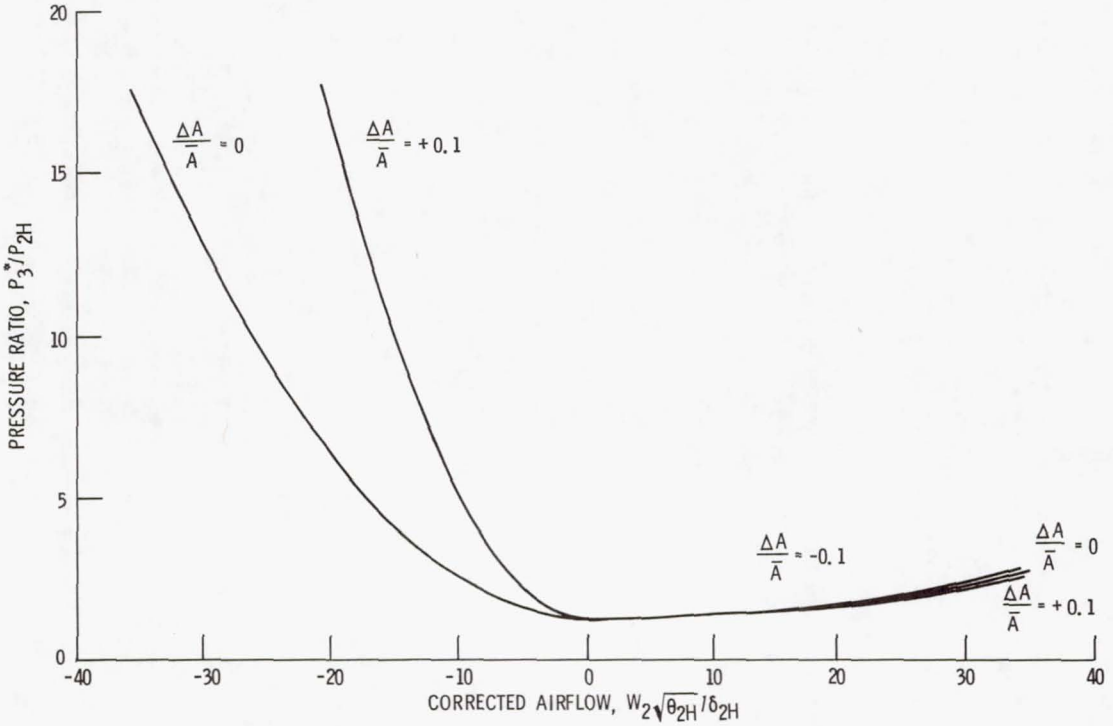

Figure 7. - In-stall compressor map showing the effect of varying KPC and KNC.

Figure 8. - Variation in recovery area as a function of radial flow resistance.